Journal of the Physical Society of Japan
Vol. 52, No. 5, May, 1983, pp. 1848–1856

# Vacuum Ultraviolet Reflectance Spectra and Band Structures of Pyrites ($FeS_2$, $CoS_2$ and $NiS_2$) and NiO Measured with Synchrotron Radiation

Shigemasa SUGA, Kouichi INOUE, Masaki TANIGUCHI, Shik SHIN, Masami SEKI, Katsuaki SATO† and Teruo TERANISHI†

*Synchrotron Radiation Laboratory, Institute for Solid State Physics, The University of Tokyo, Tanashi, Tokyo 188*
*†Broadcasting Science Research Laboratories of Nippon Hoso Kyokai, Setagaya, Tokyo 157*

(Received November 27, 1982)

Reflectance spectra of $FeS_2$, $CoS_2$, and $NiS_2$ pyrites have been measured in the photon energy region from 4 to 30 eV with synchrotron radiation and compared with the results of NiO and related compounds. Dielectric constants, optical constants, effective electron numbers as well as energy-loss functions are evaluated by means of the Kramers-Kronig analysis. Fine structures of the reflectance spectra are qualitatively interpreted providing information on band structures. Characteristic features of band structures related to the 3*d* electrons in the low-spin state are experimentally elucidated.

## §1. Introduction

Among various transition metal compounds, transition metal pyrites have attracted much interest because of their variegated electrical, optical and magnetic properties. For example, $CoS_2$ shows ferromagnetism with Curie temperature of 116 K in contrast to the paramagnetism of $FeS_2$. Meanwhile, $NiS_2$ shows antiferro- and weak ferro-magnetism.[1] Besides, $CoS_2$ shows metallic conductivity, whereas $FeS_2$ and $NiS_2$ are semiconductors with the band gap energies of about 0.8 eV[2] and 0.37 eV,[3] respectively. So far optical studies of pyrites have been limited near the band gap and in low energy regions[4] except for $FeS_2$.[5] XPS[6] and UPS[7] photoelectron spectroscopy, however, has revealed valence band structures to some extent.

The purpose of the present research is to study their electronic structures related to the low-spin configuration and itinerancy of the 3*d* electrons by synchrotron radiation spectroscopy. Measurements have been performed between 4 and 30 eV, and the results are compared with recent band calculations. We have further discussed these results in comparison with that of NiO, which is known as a typical Mott insulator with a large band gap energy and antiferro-magnetism with Néel temperature of 525 K.

## §2. Experimental

Single crystals of $CoS_2$ and $NiS_2$ were grown by chemical vapor transport technique with chlorine gas as a transport agent.[8] Untreated specular surfaces of $CoS_2$ and $NiS_2$ were used for reflectance measurements. As for $FeS_2$, we used a specular surface of a natural crystal obtained by polishing and etching. In addition, we measured reflectance of NiO and MgO single crystals, cleaved in air and in ultra-high vacuum, respectively.

We measured *p*-polarized reflectance spectra in the wavelength region from 3000 to 400 Å by use of a 1m Seya-Namioka monochromator installed at the first beam line of SOR-RING (0.4 GeV electron storage ring), with a resolution of 3 Å. Data acquisition was performed by use of a microcomputer system equipped with a minifloppy disk handler. In this experiment, we used either a $MgF_2$ or a fused quartz filter to suppress the second order light.

## §3. Results and Analysis

Figure 1(a) through Fig. 1(c) show reflectance spectra of $FeS_2$, $CoS_2$, and $NiS_2$ with the

Table I. Reflectance structures and the present interpretation for $FeS_2$, $CoS_2$ and $NiS_2$. The energies of the reflectance structures are given in eV units.

| $FeS_2$ | $CoS_2$ | $NiS_2$ | |
|---|---|---|---|
| | | 0.8 | $d\gamma \rightarrow d\gamma + p^*$ |
| 1.6 | 1.4 | 1.7 | $d\varepsilon \rightarrow d\gamma + p^*$ |
| | | 2.7 | $d\gamma \rightarrow d\gamma + p^*$ |
| 4.0 | 3.2 | 3.8 | $d\varepsilon \rightarrow d\gamma + p^*$ |
| 5.1 | 6.0 | 5.8 | $p \rightarrow d\gamma + p^*$ |
| 5.9 | | | |
| 7.4 | 7.3 | 6.2 | |
| 9.2 | 8.9 | 7.6 | $p \rightarrow (s, p)$ conduction bands |
| | | 8.2 | |
| 10.0 | 9.6 | 8.8 | |
| | | 9.4 | |
| 11.5 | 11.2 | 10.4 | |
| 12.4 | | | |
| 14.5 | 15.0 | 13.9 | $s, s^* \rightarrow d\gamma + p^*$ |
| 16.5 | 16.5 | 15.8 | |
| 19.7 | 20.0 | 18.5 | $s, s^* \rightarrow (s, p)$ conduction bands |
| | | (eV) | |

pyrite crystal structure. Experimental conditions on temperature and incidence angle of light ($\alpha$) are described in figure captions. The vertical lines indicate positions of observed structures for clarity purpose. These energies are summarized in Table I. Gross features of the reflectance spectra of $CoS_2$ and $NiS_2$ remained unchanged except for the reduced band width of several structures at liquid nitrogen temperature. The dashed curves in Fig. 1(a) and (c) show the reflectivity in the low energy region calculated from $n$ (refractive index) and $k$ (extinction coefficient) reported by Bither *et al.*[4] The dashed curve in Fig. 1(b) shows the reflectivity which is carefully remeasured by one of the authors (K.S.). The present reflectance spectra are smoothly continued to these reflectivities in the low energy region. One notices a common feature in these spectra that the reflectivity considerably decreases above 20 eV. The dip of the reflectivity of $CoS_2$ and $NiS_2$ between 4 and 6 eV in comparison with the reflectivity of $FeS_2$ is another feature of the reflectance spectra of pyrites.

Figure 1(d) shows the reflectance spectrum of NiO with rocksalt structure. The dashed line shows the previous result in the low energy region.[9] The spectrum of MgO is added in this figure by the dot-dashed line (with an arbitrary scale of ordinate), since the absence of occupied $3d$ electrons in MgO is helpful for discussing the contribution from the incompletely filled $3d$ electrons to the reflectance spectrum of NiO. One recognizes that the reflectance structures of NiO between 8 and 20 eV are rather similar to those of MgO. In the case of NiO, more structures are resolved than the previous result by Powell and Spicer[9] by virtue of the continuous synchrotron radiation source. As for MgO, the present result is not much different from the results previously reported.[10]

By means of the Kramers-Kronig transformation considering the finite incidence angle,[11] we have evaluated $N_{\text{eff}}$ (effective electron number per molecule) of $FeS_2$, $CoS_2$, $NiS_2$ and NiO in Fig. 1(a) through 1(d). Figure 2 summarizes the energy-loss function ($-\text{Im}\,(1/\varepsilon)$). Likewise, we have shown dielectric constants ($\varepsilon_1$, $\varepsilon_2$) and optical constants ($n$, $k$) in Fig. 3(a) through 3(d).

## §4. Discussion

In pyrite crystals with the space group symmetry of $T_h^6$, the transition metal ion ($M^{2+}$) is surrounded by six $S_2^{2-}$ molecules with the site symmetry represented by $S_6$. In the simplest approximation, we consider that the $M^{2+}$ ion is at the center of the six nearest neighbor sulphur atoms arranged octahedrally.[5] Then the $3d$ orbitals of the $M^{2+}$ ion are split into $d\varepsilon(t_{2g})$ and $d\gamma(e_g)$ orbitals with the $d\varepsilon$ levels in the lower energy region due to the smaller overlap with the ligand wave functions. Four $M^{2+}S_2^{2-}$ molecules are contained in a unit cell of pyrites. In rocksalt structures, the $3d$ orbitals are likewise split into $d\varepsilon$ and $d\gamma$ oribtals in $O_h$ crystal field. Rocksalt structures contain also four molecules in a unit cell.

### *4.1 Discussion on pyrites*

Here we discuss the reflectance spectra of $FeS_2$, $CoS_2$ and $NiS_2$. In the first place, we notice that the spectra of $-\text{Im}\,(1/\varepsilon)$ show peaks at 23.3, 23.0 and 21.8 eV for $FeS_2$, $CoS_2$ and $NiS_2$, respectively. Recent experiments on low-energy electron energy loss spectroscopy of these pyrites have provided bulk plasmon energies around 22.5, 23.5 and

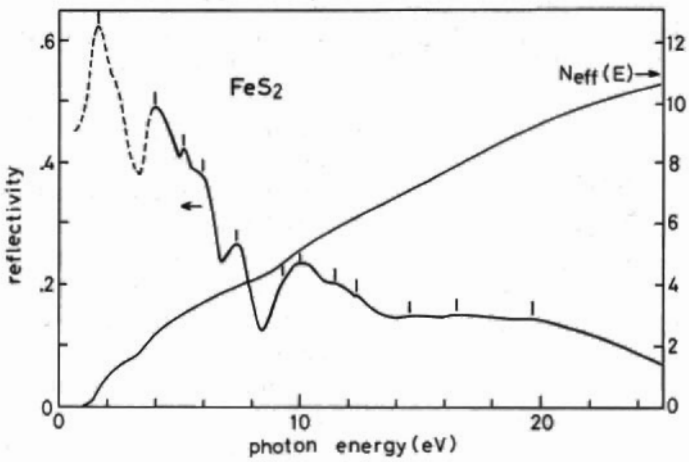
FeS2
Neff(E)
reflectivity
photon energy(eV)

(a)

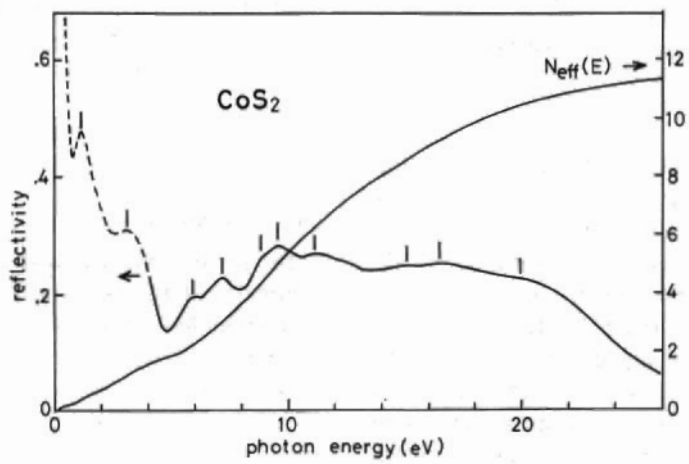
CoS2
Neff(E)
reflectivity
photon energy(eV)

(b)

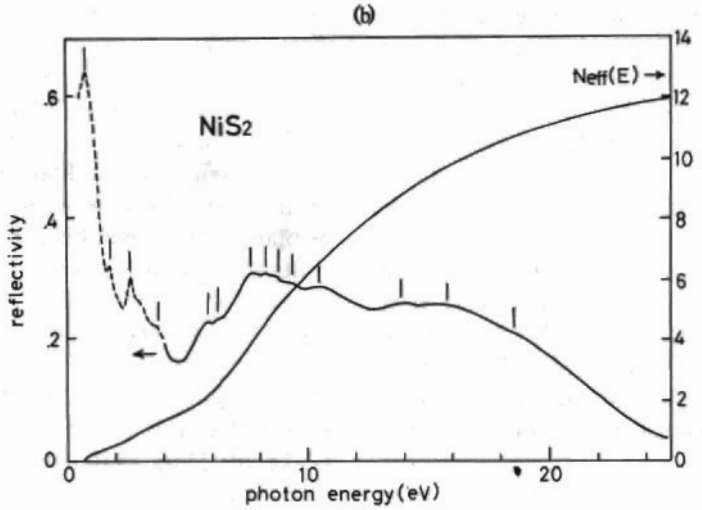
NiS2
Neff(E)
reflectivity
photon energy(eV)

(c)

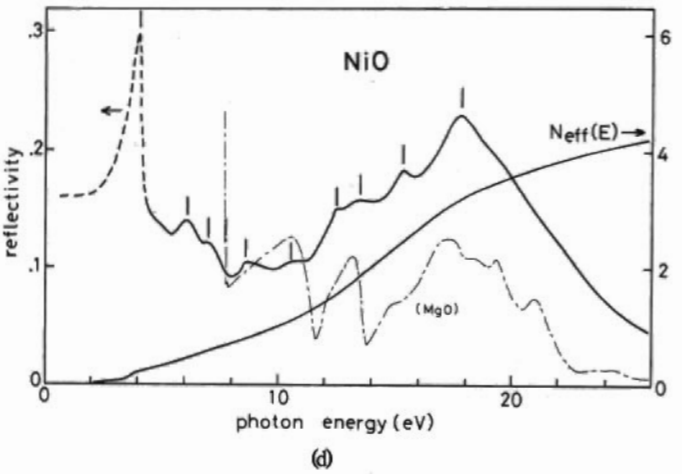


Fig. 1. Reflectance spectra and $N_{eff}$ evaluated from the Kramers-Kronig analysis. (a) reflectivity of $FeS_2$ at liquid nitrogen temperature measured at $\alpha=9°$. (b) reflectivity of $CoS_2$ at room temperature for $\alpha=12.5°$. (c) reflectivity of $NiS_2$ at room temperature for $\alpha=22.5°$. (d) reflectivity of NiO at liquid nitrogen temperature for $\alpha=10.0°$. The dot-dashed line shows the reflectance spectrum of MgO with an arbitrary scale.

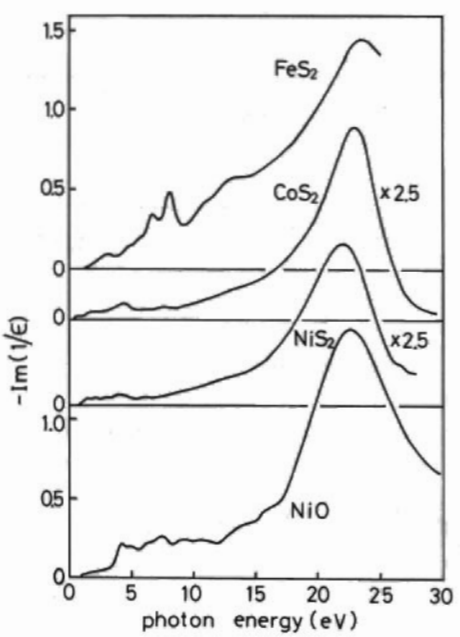


Fig. 2. Energy-loss function $-\mathrm{Im}(1/\varepsilon)$ evaluated from the Kramers-Kronig analysis. The results of $CoS_2$ and $NiS_2$ should be multiplied by 2.5.

24.0 eV.[12] Therefore we can certainly assign the gradual decrease in the reflectivity of these materials above 20 eV to the plasma edge. The slight discrepancy between these two energies in the case of $NiS_2$ may be due to an underestimate of the reflectivity, possibly induced by an inappropriate continuation of the spectrum to the low energy data.

The band calculation of pyrites has been recently performed by *KKR* method,[13] where the density of states is also given by *LCAO* extrapolation. Figure 4(a), (b), and (c) show the density of states of $FeS_2$, $CoS_2$ and $NiS_2$, where the vertical arrows give the Fermi energies ($E_F$). The characteristics of the calculated band structures of pyrites are summarized as follows:

1) In the lowest energy region are lying isolated bands mainly composed of bonding ($s$) and antibonding ($s^*$) orbitals of the $S_2^{2-}$ $3s$ states.

2) Just below the Fermi level are placed occupied bands with small dispersion resulting from $M^{2+}$ $3d$ orbitals. In pyrites, the $d\gamma$ bands are considerably hybridized with $S_2^{2-}$ antibonding $p^*$ orbitals due to the covalency, in contrast to the nonbonding character of the $d\varepsilon$ bands. Since the $3d$ electrons of pyrites are in the low-spin configuration, the topmost filled band corresponds to $d\varepsilon$ bands in $FeS_2$ and to $d\gamma+p^*$ hybridized bands in $CoS_2$ and $NiS_2$. Namely, the $d\gamma+p^*$ bands are empty in $FeS_2$ and partially filled in $CoS_2$ and $NiS_2$.

3) Below these $3d$ bands are situated the $p$ valence bands mainly composed of the $p$ bonding orbitals of $S_2^{2-}$ molecule. The upper

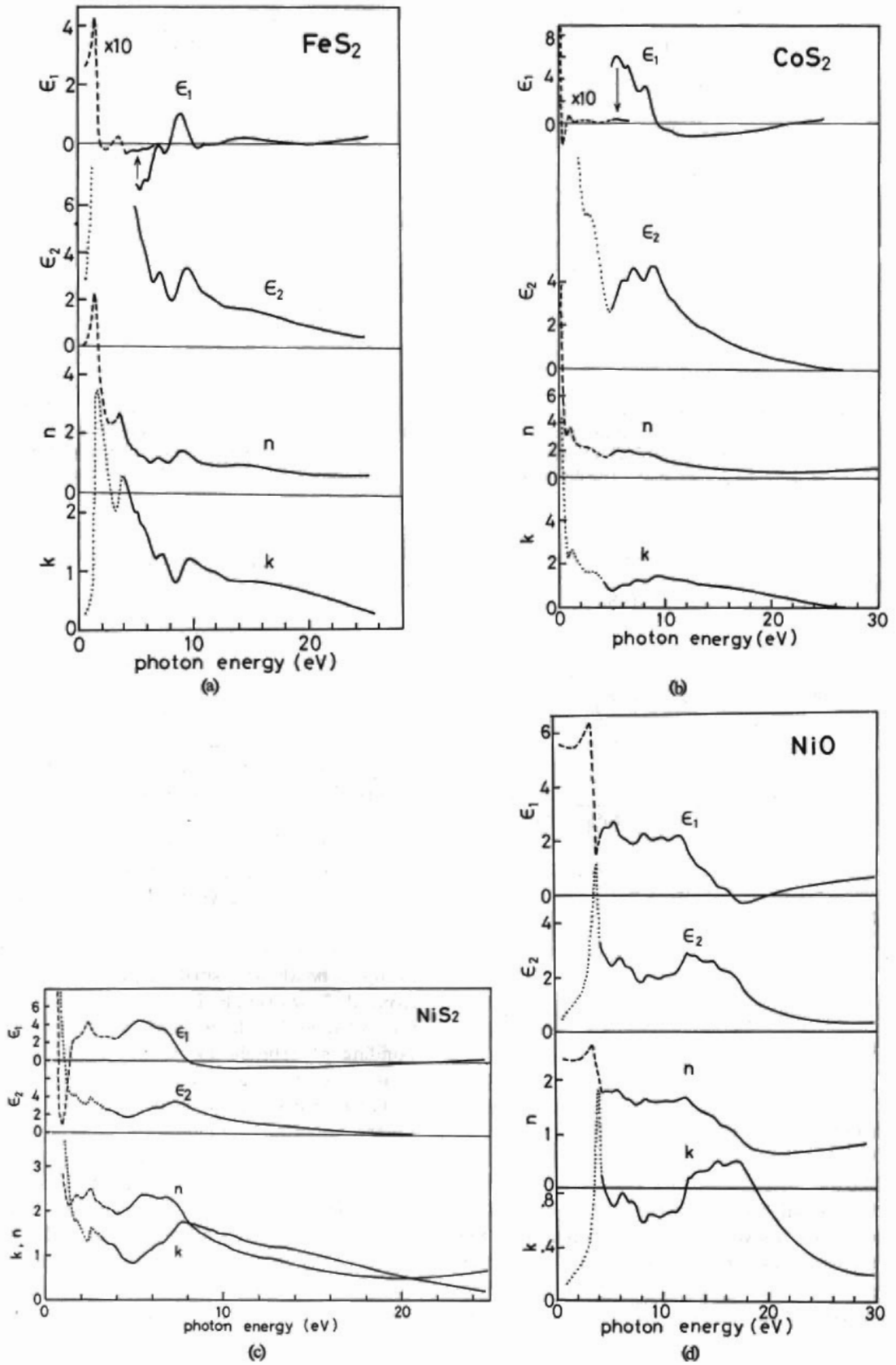


Fig. 3. Dielectric constants and optical constants of (a) $FeS_2$ (b) $CoS_2$ (c) $NiS_2$ and (d) NiO.

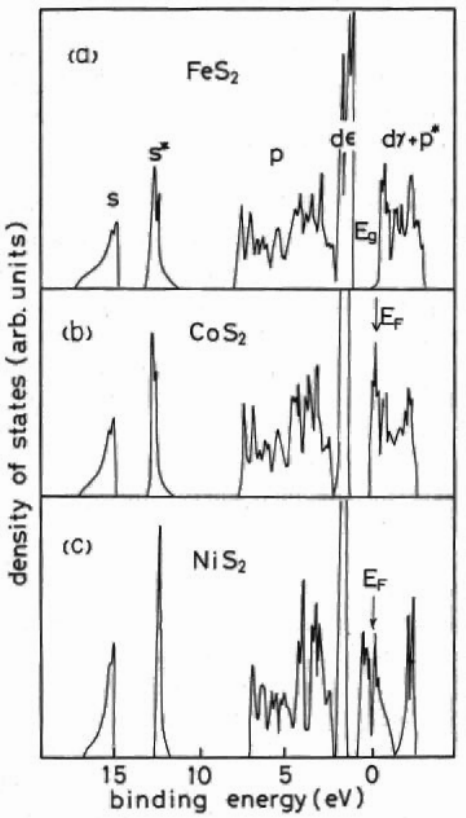


Fig. 4. Density of states of pyrites according to band calculation in non-magnetic phase by S. Asano [13]. (a) $FeS_2$ (b) $CoS_2$ and (c) $NiS_2$.

parts of these $p$ bands are hybridized with the $M^{2+}$ $3d$ orbitals to some extent.

The *XPS* experiment has revealed the *EDC* structure related to the sulphur $3s$ orbitals around 13 eV[6] below the top of the occupied band. Considering the small band gap of $FeS_2$ and $NiS_2$ and the metallic character of $CoS_2$, the optical transition from the deep $3s$ valence bands to conduction bands will take place above 13 eV. The broad reflectance structures of these pyrites above 13 eV are most likely assigned to the transitions from these $3s$ bands. The dipole allowed transitions from sulphur $3s$ to sulphur $3p$ levels are observable in pyrites, because the antibonding $3p^*$ orbitals of the $S_2^{2-}$ contribute much to the conduction bands. In addition, we can expect a considerable hybridization (covalency) of $S_2^{2-}$ $3p$ orbitals with $M^{2+}$ $3d$ (in particular, $d\gamma$) orbitals near the band gap or band edge region. These results are the characteristic features of pyrites in contrast to ionic transition metal compounds such as mono-oxides.

Considering the high density of states of $s$ and $s^*$ bands and the $p^*$ character of the conduction bands, the reflectance structures at 14.5 and 16.5 eV in $FeS_2$, at 15.0 and 16.5 eV in $CoS_2$ and at 13.9 and 15.8 eV in $NiS_2$ are surely assigned to the $s, s^* \rightarrow d\gamma + p^*$ transitions as proposed before. Hereafter we discuss energy positions of reflectance peaks, since the structures are less obvious in the $\varepsilon_2$ spectra. We consider that the splitting between the $s$ and $s^*$ bands corresponds to the observed splitting between these two structures. The origin of the faint structure in the highest energy region may be due to transitions to higher $(s, p)$ conduction bands. According to this interpretation, the $(s, p)$ conduction bands are situated around 5 eV above the $d\gamma + p^*$ bands. The $N_{\text{eff}}$ at 25 eV shown in Fig. 1 are much smaller than the values of 20, 21 and 22 expected for the electron configuration of $M^{2+}(3d^m)S_2^{2-}(3s^4 3p^{10})$ with $m=6$, 7 and 8 for $FeS_2$, $CoS_2$ and $NiS_2$. The increment of $N_{\text{eff}}$ between 13 and 25 eV is, however, around 4 in support of the before-mentioned assignment of $s, s^* \rightarrow d\gamma + p^*$ and $(s, p)$ conduction bands in this energy region. These results also elucidate that the transitions from the $p$ valence bands continue slightly beyond $h\nu =$ 25 eV and that the transitions from occupied $d$ bands are not playing dominant contributions in the present spectra except for the low energy structures below 4 eV as shown below.

In the case of $FeS_2$, the band structure is rather simple as demonstrated in Fig. 4(a), because the filled $d\varepsilon$ bands are separated from the $d\gamma + p^*$ conduction bands by the band gap. In this case the reflectance peak at 1.6 eV is assigned to the transition from the rather narrow $d\varepsilon$ bands to the low energy region of the $d\gamma + p^*$ bands. Considering the band width of the $d\gamma + p^*$ conduction bands of about 2.5 eV, we assign the next reflectance peak at 4.0 eV as well to the excitation from $d\varepsilon$ to the high energy region of $d\gamma + p^*$ bands. Taking the band widths of the $p$ and $d\gamma + p^*$ bands into account, the next reflectance structures of $FeS_2$ below 8.5 eV (the energy corresponding to a reflectance minimum) are most likely assigned to the $p \rightarrow d\gamma + p^*$ excita-

tion. This excitation is expected to continue down to around 3 eV (Fig. 4) in the lower energy region and to overlap with the before-mentioned $d\varepsilon \rightarrow d\gamma + p^*$ excitation.

In the case of $CoS_2$, the peak at 1.4 eV has been assigned to $d\varepsilon \rightarrow d\gamma + p^*$.[8] According to the band structure shown in Fig. 4(b), the peak at 3.2 eV can be also assigned to the $d\varepsilon \rightarrow d\gamma + p^*$ excitation. Meanwhile the structures between 4 and 8 eV are interpreted as due to the $p \rightarrow d\gamma + p^*$ excitation which may extend down to 3 eV. One may generally expect that the transition intensity from the $p$ valence bands to the $d\gamma + p^*$ conduction bands should decrease in accordance with the decrease of the number of the empty $d\gamma$ states. Thus the structures below 8 eV of $FeS_2$ and $CoS_2$ and the corresponding structures of $NiS_2$ below 7 eV are assigned to this transition. This is a characteristic manifestation of the low-spin configuration of $3d$ electrons in pyrites.

As for $NiS_2$, there occur remarkable dips of the density of states in the middle of the $d\gamma + p^*$ conduction bands and around $E_F$ as shown in Fig. 4(c). In fact, $NiS_2$ has a small gap due to the electron correlation effect as well known for Mott insulators.[1,3] Thus, one expects that both $d\gamma \rightarrow d\gamma + p^*$ and $d\varepsilon \rightarrow d\gamma + p^*$ excitations are separately observable in $NiS_2$. We are tempted to assign the reflectance structures reported at 0.8 and 2.7 eV[4] to the $d\gamma \rightarrow d\gamma + p^*$ excitation and the structures at 1.7 and 3.8 eV to $d\varepsilon \rightarrow d\gamma + p^*$ transition, respectively.

Since the $d\gamma$ character is dominant in the lower energy part of the $d\gamma + p^*$ bands of $CoS_2$ and $NiS_2$,[13] the $p \rightarrow d\gamma + p^*$ excitation terminates in this part of the $d\gamma + p^*$ conduction bands. The decrease in the energy of the reflectance minimum corresponding to the high energy limit of the $p \rightarrow d\gamma + p^*$ excitation from $FeS_2$ to $NiS_2$ is partly due to the reduction of the total band width of the $p$ valence bands in this order. Meanwhile, the low-spin configuration of the $3d$ electrons in pyrites suggests that the crystal field splitting energy $10Dq$ of $Fe^{2+}$, $Co^{2+}$ and $Ni^{2+}$ is much larger than the corresponding value in high-spin materials. For example, it was evaluated for high-spin di-halide compounds as 1.28 eV, 1.04 eV and 1.02 eV.[14] The crystal field splitting of the $3d$ electrons in pyrites is, however, very difficult to evaluate due to the considerable energy dispersion or band width of the $d\gamma$ bands caused by the hybridization with the $p^*$ orbitals. $10Dq$ in pyrites are tentatively evaluated as 1.6 eV, 1.4 eV and 1.7 eV in $FeS_2$, $CoS_2$ and $NiS_2$, respectively, from the energies of the reflectance peak assigned to $d\varepsilon \rightarrow d\gamma + p^*$ transition. In the case of $FeS_2$, $10Dq$ is better evaluated as 2.5 eV from the analysis of the multiplet structures due to the $3p$ core excitation.[15] The strong covalency of the $d\gamma$ and $p^*$ orbitals is also ascertained by the evaluation of the reduction factors of the Slater-Condon parameters.[15]

Between the high energy threshold of the $p \rightarrow d\gamma + p^*$ excitation and the low energy threshold of $s, s^* \rightarrow d\gamma + p^*$ excitation structures, fairly strong reflectance structures are observed in all pyrites. Considering the energy position and the band width of the reflectance structures, these transitions are most likely attributed to the excitation from the $p$ valence bands to the $(s, p)$ conduction bands. This assignment provides the energy position of the $(s, p)$ conduction bands around $5 \sim 7$ eV above the $d\varepsilon$ band (Table I), which is consistent with the before-mentioned energy position of the $(s, p)$ conduction bands.

### *4.2 Discussion on NiO*

In the case of NiO, the O $2s$ band is placed about 21 eV below the top of the valence band according to the results of *XPS* measurement.[16] Besides, NiO is an insulator with a band gap energy of around 4 eV.[17] Therefore, the strong reflectance structures of NiO observed in the energy region between 12 and 20 eV can not be assigned to the transitions resulting from the O $2s$ bands. Moreover, one expects smaller degree of hybridization between the O $2p$ and Ni$3d$ orbitals in large gap NiO in comparison with narrow gap or metallic pyrites.[18] Therefore, an observation of the transition from the O $2s$ bands to the lowest conduction band is difficult in NiO according to the less component of the O $2p$ orbitals in the conduction bands. We have already pointed out that the gross feature of the strong reflectance structures of NiO and MgO between 8 and 20 eV is very similar to each other. The

reflectance structures around 13 and 18 eV are likewise observable in other II-VI oxide compounds such as CaO,[19] CdO, BeO and ZnO.[20] Here CaO and CdO have rocksalt structure and both BeO and ZnO have wurtzite structure. Among these crystals, BeO, MgO, and CaO have no occupied $d$ level, whereas ZnO and CdO have completely filled $3d$ and $4d$ levels far below the top of the valence bands. Meanwhile, NiO has incompletely filled $3d$ levels at the top of the valence bands. The similarity of the reflectance structures around 13 and 18 eV observed in all of these materials irrespective of the occupation condition of the $d$-levels, however, suggests that the structures of NiO in this energy region can not be attributed to the transition from the Ni $3d$ occupied levels.

In Fig. 1(d), $N_{\text{eff}}$ in NiO is evaluated to be around 4.2 at 25 eV, which is much smaller than $N_{\text{eff}}=14$ expected from the electron configuration of $Ni^{2+}(3d^8)O^{2-}(2p^6)$. This result elucidates that the transitions from O $2p$ and Ni $3d$ orbitals to conduction bands continue far beyond $h\nu=25$ eV. In this regard, $N_{\text{eff}}$ of MgO, CdO, and ZnO are evaluated as 4.4,[11] 5.4,[20] and $5\sim6$[20] at 25 eV, which are consistent with the present interpretation.

According to the pseudopotential band calculation of MgO,[21] the reflectance structures of MgO shown in Fig. 1(d) have been assigned to interband transitions characterized by O $2p\rightarrow(s,p)$ conduction bands excitations and accompanying excitons. Judging from the similarity of the reflectance structures of NiO with those of MgO, most part of the reflectance structures of NiO between 8 and 20 eV is likewise interpreted as due to O $2p\rightarrow(s,p)$ conduction bands. This result shows that the band gap between the O $2p$ valence bands and the $(s,p)$ conduction bands in NiO neglecting the Ni $3d$ orbitals is comparable to that of MgO. With respect to the structures of NiO below 8 eV, which have no counterpart in MgO, we consider the following possibilities:[9,22,23] (1) transitions from the O $2p$ valence bands to the empty $d\gamma$ orbitals of Ni, (2) transitions from occupied $d\varepsilon$ and $d\gamma$ orbitals to the $(s,p)$ conduction bands, (3) excitation of partially filled $Ni^{2+}$ $3d^8$ electrons as $2(3d^8)\rightarrow3d^9+3d^7$.

First, the structures of NiO around 6 and 7 eV are much weaker than the corresponding structures in MnO.[23] Therefore, we prefer the first possibility (O $2p\rightarrow d\gamma$) for the interpretation of these structures in NiO, as in the case of pyrites. According to our recent investigation,[24,18] we should also consider the intra-atomic $d$-$d$ correlation energy to explain the correct energy positions of these excitations.

Second, the structure at 4 eV in NiO can be assigned to the excitation from the occupied $d$ levels to the bottom of the $(s,p)$ conduction bands (second possibility as shown before) according to the recent band calculation.[17] The intensity of this transition is much larger than that in MnO with less population of the $d$ levels in the ground state, in support of the present interpretation.

As for the third possibility, the excitation energy strongly depends upon the $d$-$d$ correlation energy.[9,17,22,23] It is very unlikely that this $d\rightarrow d$ excitation provides such a strong intensity as observed for the 4 eV peak, although it may appear in the present energy region as weak structures. Thus the present interpretation of the optical spectrum of NiO is consistent with those of pyrites.

## §5. Conclusion

As a conclusion, we measured reflectance spectra of $FeS_2$, $CoS_2$, $NiS_2$ and NiO in the energy region between 4 and 30 eV by use of synchrotron radiation. The spectra are analyzed by the Kramers-Kronig transformation providing evaluation of dielectric constants, optical constants, energy-loss function as well as effective electron numbers. The whole reflectance structures below 30 eV of $FeS_2$, $CoS_2$ and $NiS_2$ are qualitatively interpreted on a basis of a recent band calculation. Controversial interpretation of reflectance spectra of various transition metal compounds are settled in pyrite compounds. The band structures due to the antibonding as well as bonding orbitals of $3s$ electrons of $S_2$ molecule are definitely resolved in reflectance spectra. The decrease in the reflectivity above 20 eV is identified as the plasma edge according to the evaluated $\varepsilon_1$, $\varepsilon_2$ and $-\text{Im}\,(1/\varepsilon)$. The reflectance structures in the lower energy region are

assigned as follows:

1) Transitions from the $p$-like valence bands to higher conduction bands with $s$ character correspond to the structures between 8 and 13 eV in $FeS_2$ and $CoS_2$ and between 7 and 13 eV in $NiS_2$. These transitions correspond to the structures between 8 and 20 eV in NiO.

2) Transitions from the $p$-like valence bands to the lowest conduction bands characterized by $d\gamma+p^*$ hybridized orbitals, correspond to the structures between 3 and 8 eV in $FeS_2$ and $CoS_2$ and between 3 and 7 eV in $NiS_2$. The decrease of the transition intensity of this excitation in the order of $FeS_2$, $CoS_2$ and $NiS_2$ is a characteristic feature of the low-spin configuration of the $3d$ electrons in pyrites.

3) Transitions from the $d\varepsilon$ valence bands to the lowest conduction bands are attributed to the structures below around 4 eV in $FeS_2$, $CoS_2$ and $NiS_2$.

In order to derive direct information about valence band structures, an angle resolved UPS experiment will be very fruitful. In addition, inner core excitation spectroscopy of these pyrites provides further information about band structures, covalency and final state interactions in the excited states.

## Acknowledgment

The authors are much obliged to Professor H. Kanzaki and colleagues of Synchrotron Radiation Laboratory and to the staff of Computer Facility of Institute for Nuclear Study for continuous supports during the experiment. They are grateful to Dr. K. Ohsumi of Department of Mineralogy, The University of Tokyo for providing us single crystal $FeS_2$. They thank Professor S. Asano for allowing us to cite the results of his band calculation before publication. This work was partly supported by Grant-in Aid for Scientific Research (Grant No. 354072) of the Ministry of Education, Science and Culture of Japan.

## References

1) S. Ogawa: J. Appl. Phys. **50** (1979) 2308; S. Ogawa: Solid State Phys. **12** (1977) 657 [in Japanese]; K. Adachi: *ibid.* **10** (1975) 101 [in Japanese].
2) W. W. Kou and M. S. Seehra: Phys. Rev. **B18** (1978) 7062.
3) R. L. Kautz, M. S. Dresselhaus, D. Adler and A. Linz: Phys. Rev. **B6** (1972) 2078.
4) T. A. Bither, R. J. Bouchard, W. H. Cloud, P. C. Donohue and W. J. Siemons: Inorg. Chem. **7** (1968) 2208.
5) A. Schlegel and P. Wachter: J. Phys. **C9** (1976) 3363.
6) A. Ohsawa, H. Yamamoto and H. Watanabe: J. Phys. Soc. Jpn. **37** (1974) 568.
7) E. K. Li, K. H. Johnson, D. E. Eastman and J. L. Freeouf: Phys. Rev. Lett. **32** (1974) 470.
8) K. Sato and T. Teranishi: J. Phys. Soc. Jpn. **50** (1981) 2069.
9) R. J. Powell and W. E. Spicer: Phys. Rev. **B2** (1970) 2182.
10) D. M. Roessler and W. C. Walker: Phys. Rev. **159** (1967) 733; M. W. Williams and E. T. Arakawa: J. Appl. Phys. **38** (1967) 5272.
11) CPC Program, ACKD, Institute for Nuclear Study, The University of Tokyo.
12) K. Sato *et al.*: to be published.
13) S. Asano: private communication.
14) S. Shin, S. Suga, M. Taniguchi, H. Kanzaki, S. Shibuya and T. Yamaguchi: J. Phys. Soc. Jpn. **51** (1982) 906.
15) S. Suga, M. Taniguchi, S. Shin, M. Seki, S. Shibuya, K. Sato and T. Yamaguchi: *Proc. 16th Int. Conf. Phys. Semicond. Montpellier, 1981*, Physica **117B** & **118B** (1983) 353.
16) G. K. Wertheim and S. Hufner: Phys. Rev. Lett. **28** (1972) 1028.
17) A. B. Kunz: J. Phys. **C14** (1981) L455.
18) S. Suga, S. Shin, M. Taniguchi, K. Inoue, M. Seki, I. Nakada, S. Shibuya and T. Yamaguchi: Phys. Rev. **B25** (1982) 5486.
19) R. C. Whited and W. C. Walker: Phys. Rev. **188** (1969) 1380.
20) J. L. Freeouf: Phys. Rev. **B7** (1973) 3810.
21) C. Y. Fong, W. Saslow and M. L. Cohen: Phys. Rev. **168** (1968) 992.
22) C. R. Catlow and D. G. Muxworthy: Philos. Mag. **B37** (1978) 63.
23) L. Messick, W. C. Walker and R. Glosser: Phys. Rev. **B6** (1972) 3941.
24) S. Shin, S. Suga, M. Taniguchi, M. Seki, H. Kanzaki, Y. Ueda, K. Kosuge and S. Kachi: to be published.